

Thermoelectric properties of a very-low-mobility two-dimensional electron gas

R. Fletcher

Physics Department, Queen's University, Kingston, Ontario, Canada K7L 3N6

J. J. Harris

*Electronic and Electrical Engineering, University College, London WC1E 7JE, United Kingdom
and Semiconductor Interdisciplinary Research Centre, Imperial College, London SW7 2BZ, United Kingdom*

C. T. Foxon

Department of Physics, University of Nottingham, Nottingham N97 2RD, United Kingdom

M. Tsaousidou and P. N. Butcher

Department of Physics, University of Warwick, Coventry CV4 7AL, United Kingdom

(Received 29 July 1994)

Experimental data on the thermoelectric coefficients of a very-low-mobility ($\mu=0.13$ m²/V s) two-dimensional electron gas in a GaAs/Ga_{1-x}Al_xAs quantum well are presented. The measurements span a temperature range of 1–200 K, and have been made in magnetic fields up to 8 T (at which point $\omega\tau\sim 1$). As with high-mobility samples, phonon drag is found to be dominant at low temperatures, showing that the sample mobility is not relevant to this quantity. Data on the thermopower $S_{xx}(B)$ and the Nernst-Ettingshausen coefficient $S_{yx}(B)$ are compared with recent theoretical predictions. In the absence of magnetic field, $B=0$, the phonon mean free path (mfp) is initially determined from the measured thermal conductivity. Then the calculated value of $S_{xx}(0)$ (thermopower in zero field) is in good agreement with measured values when $T < 10$ K but becomes up to an order of magnitude too small when $T > 20$ K. To avoid this problem when $B \neq 0$ the phonon mfp is redetermined from the measured values of $S_{xx}(0)$ with the diffusion part subtracted. Then the calculated magnetothermopower $\Delta S_{xx}(B)$ is in good agreement with the data. The calculated drag contribution $S_{yx}^g(B)$ to the Nernst-Ettingshausen coefficient $S_{yx}(B)$, however, is only 5.4% of that measured. When the theoretical value of the contribution to $S_{yx}(B)$ due to phonon drag is increased by a factor of $(0.054)^{-1} = 18.5$ for all B and T , very good agreement with the data is again obtained over the whole regime investigated experimentally.

I. INTRODUCTION

The thermopower of two-dimensional electron gases (2DEG's) has recently been reviewed by Gallagher and Butcher¹ and their paper should be consulted for extensive citations to much of the work that will be briefly summarized here. The thermopower tensor \vec{S} is defined by $\mathbf{E} = \vec{S}\nabla T$, where \mathbf{E} is the electric field and ∇T is the temperature gradient. Extensive experimental data are available on \vec{S} at both zero and nonzero magnetic field. Measurements have been made on both heterostructures and Si metal-oxide-semiconductor field-effect transistors, but this discussion will be restricted to heterostructures, and will be particularly concerned with GaAs/Ga_{1-x}Al_xAs systems. When a magnetic field \mathbf{B} is present along \hat{z} and a temperature gradient along \hat{x} there are two independent components of \vec{S} [$S_{xx}(B)$ and $S_{yx}(B)$] that can be measured. The earliest experiments concentrated on S_{xx} , both with and without a magnetic field, but later investigations examined both components. Except for some recent measurements² on a series of GaAs/Ga_{1-x}Al_xAs heterostructures up to 200 K, all of the experimental and theoretical work is restricted to low temperatures, roughly the ⁴He range and below.

Early measurements appeared to be consistent with the theories at the time, most of which were concerned with

the behavior of $S_{xx}(B)$ at high magnetic fields where quantum oscillations are seen, and all of which treated only the diffusion component $S_{xx}^d(B)$ and ignored the phonon drag part $S_{xx}^g(B)$. In contrast, later experimental and theoretical work, both with and without a magnetic field, are all consistent with a very large phonon-drag contribution, in fact usually so large that S_{xx}^d would not be visible unless the measurements were extended to very high or very low temperatures. Because there was a progression from low-mobility to high-mobility structures (roughly from 2–50 m²/V s) in the same time period, one might be tempted³ to conclude that the magnitude of S_{xx}^g increases as the mobility increases. However, the mobility should not play a major role in the phonon-drag component. In bulk conductors S_{xx}^g usually drops when the mobility is reduced or adding impurities to the crystal. This is not caused by the reduction in mobility as such, but rather arises because the phonons are scattered by the impurities to a greater or lesser extent, which reduces the available phonon momentum, which can be transferred to the electrons. In the 2DEG case the impurities are essentially local to the electrons, rather than being in the bulk of the substrate, and should therefore have little effect on the phonons. The sample we have investigated in the present work has a mobility μ of about 0.13 m²/V s, which is at least an order of magnitude lower than those

used in the early experiments and is meant to provide a definitive experimental test of whether phonon drag is noticeably reduced by low mobility.

A low-mobility sample offers other interesting possibilities. Our sample is in the low-field regime up to the maximum available field of 8 T ($\omega\tau \sim 1$, with ω the cyclotron frequency and τ the quantum lifetime), and so exhibits no quantum oscillations. Under these conditions the diffusion components $S_{ij}^d(B)$ are readily calculated, especially for only a single subband. The mobility of the present sample is so low that impurity scattering dominates phonon scattering at all temperatures accessible to this study ($T < 200$ K), thus simplifying the analysis. A further unusual feature about this sample is its very high carrier density ($n = 3.6 \times 10^{16} \text{ m}^{-2}$), which gives a high degeneracy temperature ($T_F \approx 1400$ K). Thus the low-temperature approximations for $S_{ij}^d(B)$ will remain valid to high temperatures, a useful result when trying to untangle diffusion and phonon-drag contributions. Conventional theories¹ have had difficulty in predicting the behavior and magnitude of the transverse-phonon-drag thermopower $S_{yx}^g(B)$ (usually called the Nernst-Ettingshausen coefficient). In the quantum and fractional quantum Hall regime there is experimental evidence that the measured $S_{yx}(B)$ cannot be explained by diffusion alone, and in fact is probably dominated by phonon drag. A recent theory⁴ indicates how this might arise, and, in particular, might explain the oscillations of $S_{yx}(B)$ about zero that are observed in some samples. The data presented here are measured in the low-field regime and free from oscillations. A theory of phonon drag and diffusion thermopower in this regime has been developed recently by Zianni, Butcher, and Kearney.⁵ Their analysis provides a background to the interpretation of the data in this paper. We find that the predicted drag contribution to the Nernst-Ettingshausen coefficient is too small by a factor of 0.054. After scaling the theoretical results by the empirical factor $(0.054)^{-1}$ the theory is in good agreement with the data when $0 \leq B \leq 8$ T and $0 < T \leq 200$ K.

II. EXPERIMENTAL TECHNIQUES

The sample (kindly supplied by Philips Research Laboratories, Redhill, U.K.) has a 2DEG that is confined to a single 100-Å quantum well. The mobility was strongly reduced by inserting a δ -doped plane of Si donors midway in the well. Harris, Murray, and Foxon⁶ have published the galvanomagnetic and optical properties of a series of such samples with various well widths and doping. The present sample was cleaved from the same wafer as one of these and was designated as G958 in this previous work. Reference should be made there for details of the structure. The sample is a standard Hall bar with NiAuGe contacts; the substrate dimensions are $10 \times 4.3 \times 0.51 \text{ mm}^3$. This particular sample was chosen from the series for the present experiments because it has only a single subband occupied. It was examined only under dark conditions. Thermopower measurements were made over a wide temperature range using techniques similar to those described elsewhere.² The follow-

ing outlines procedures specific to the present experiments, particularly with respect to the measurement of the temperature and temperature gradient.

The range $0.3 < T < 7$ K was covered in a ³He cryostat using a matched pair of Dale surface-mount resistors (epoxied to the sample) as the temperature-sensing elements. The effect of a magnetic field on these resistors is known in detail. For work above ~ 6 K the sample was remounted in another cryostat, which could use either liquid ⁴He or N₂ as a refrigerant. In addition, the Dale resistors were replaced by a matched pair of 2.2-k Ω Allen Bradley $\frac{1}{8}$ W resistors with usable temperature sensitivity up to about 200 K, the upper limit of our experiments. These were not calibrated in a magnetic field, though the magnetoresistance effects were clearly small at all temperatures of interest. Various temperature calibrations were available. Below 7 K we used a calibrated Ge resistor (Lakeshore Cryogenics), and between 1.5–75 K a different calibrated Ge resistor (Cryocal); the scales of these were found to accurately agree with each other in the overlap region, and also to agree with the ⁴He vapor scale to better than 10 mK. Above ~ 63 K (the triple point of N₂) a Au+0.07% Fe thermocouple was used. There are no significant discontinuities in the data in the overlap ranges, even though the lowest range had a different set of resistors so the distance between them was different. At $T > 4$ K, the temperature of the sample platform was held constant during the magnetic-field sweeps using a capacitance as the temperature-sensing element.

The temperature sensors (Dale or Allen-Bradley) were calibrated on each cooldown though both types were very reproducible. At their upper limits of temperature (7 or 200 K), the sensitivities become very small. The Allen-Bradley resistors showed some hysteresis if the temperature was cycled over a large range. This was a problem only at high temperatures and was circumvented by taking data and calibrations with temperature monotonically increasing. These effects were small, but to put them in perspective, their resistance at 200 K is about 2.7 k Ω and the change in resistance with and without a temperature gradient on the sample was about 4 Ω ; thus a resolution of 0.05 Ω was needed to obtain an accuracy approaching 1% for the temperature gradient. One problem that must be mentioned is that at the highest temperatures the application of a magnetic field of 8 T causes a change in the resistances of the Allen-Bradley resistors, which is not quite the same for each of them. This does not appear to be a simple magnetoresistance effect since it becomes noticeable only above about 150 K. Because of this it is difficult to be certain that there is no change in the temperature gradient with field to better than about 5% accuracy, but we have assumed no change in keeping with the observations at lower temperatures. The thermal conductivity of the GaAs substrate is shown in Fig. 1; above about 30 K (where boundary effects become negligible) the results are in excellent agreement with earlier data.^{7,8}

All thermoelectric data were taken using dc methods. The voltage signals were small, sometimes less than 0.1 μV [particularly for $S_{yx}(B)$], and to enable them to be

resolved accurately during the field sweeps a technique was developed to allow for drift in the zero (i.e., the voltage with no temperature gradient). As the data were being recorded by a computer, the heater producing the gradient was periodically turned off; the thermal-equilibrium time constant was very fast at low temperatures, but by 200 K had increased to about 10 sec. This technique leaves small gaps in all the results, which are noticeable on some of the figures. The variation of the zero with field was later fitted by a straight line (sometimes a quadratic) and the resulting curve subtracted from all the data. The final resolution in voltage differences is 5–10 nV.

With all measurements in a magnetic field, results were taken with both directions of the field to eliminate unwanted admixtures of the thermopower components. This was essential with $S_{yx}(B)$, but was probably unnecessary for $S_{xx}(B)$. The sample was in the shape of a Hall bar and had three pairs of transverse contacts that were available for $S_{yx}(B)$. Each pair showed a different admixture of $S_{xx}(B)$, but after the appropriate data subtractions $S_{yx}(B)$ was the same for all cases; this was checked at temperatures near 4 and 150 K. This also suggests that the transverse distances between the contact pads are the same for all pairs, which is consistent with our assumption that the relevant distance for converting the measured voltages to electric fields is the distance between the inside edges of the pads. In this sense the overall dimensions of the 2DEG are $1.5 \times 1.0 \text{ mm}^2$.

Providing we have correctly identified the appropriate length between the voltage contacts, the overall absolute accuracy of the thermoelectric coefficients should be about 5% over most of the temperature range; the relative accuracy for field sweeps up to 8 T should be better than this, and is probably about 2–3%, except possibly for the range above $\sim 150 \text{ K}$ as noted above.

III. THEORY

In the presence of an electric field \mathbf{E} (actually the negative of the gradient of the electrochemical potential) and temperature gradient ∇T , the current density \mathbf{J} in the 2DEG has two components

$$\mathbf{J} = \vec{\sigma} \mathbf{E} - \vec{\epsilon} \nabla T, \quad (1)$$

where $\vec{\sigma}$ and $\vec{\epsilon}$ are the conductivity and thermoelectric tensors, respectively. Thus the measured thermopower (with $\mathbf{J}=0$) is given by $\vec{S} = \vec{\sigma}^{-1} \vec{\epsilon}$ so that $S_{xx} = \rho_{xx} \epsilon_{xx} - \rho_{yx} \epsilon_{yx}$ and $S_{yx} = \rho_{yx} \epsilon_{xx} + \rho_{xx} \epsilon_{yx}$, where $\vec{\rho} = \vec{\sigma}^{-1}$ is the resistivity tensor and the 2DEG is assumed to be isotropic in the xy plane. The diffusion part of $\vec{\epsilon}$ may be calculated using the Mott⁹ relation $\vec{\epsilon}(\mathbf{B}) = -L_0 T e [\partial \vec{\sigma}^\dagger(-\mathbf{B}) / \partial E]_{E_F}$, where $\vec{\sigma}^\dagger$ is the transpose of $\vec{\sigma}$, L_0 is the Lorenz number $\pi^2 k_B^2 / 3e^2$, e is the magnitude of the electron charge, k_B is the Boltzmann constant, and E is the electronic energy (with E_F the Fermi energy). This is a low-temperature approximation ($k_B T \ll E_F$), which is valid only for elastic

scattering. Both of these requirements should be met with the present sample up to at least room temperature. With these relations, and using the standard expressions for the components of $\vec{\sigma}$, the diffusion contributions to \vec{S} are found to be

$$S_{xx}^d(B) = S_{xx}^d(0) + \Delta S_{xx}^d(B), \quad (2a)$$

with

$$\Delta S_{xx}^d(B) = C_d \frac{p\beta^2}{1+\beta^2} \quad (2b)$$

and

$$S_{xx}^d(0) = -(p+1)C_d. \quad (2c)$$

Finally,

$$S_{yx}^d(B) = -C_d \frac{p\beta}{1+\beta^2}. \quad (2d)$$

In these equations $p = (\partial \ln \tau / \partial \ln E)_{E_F}$, $\beta = \omega \tau$ with $\omega = eB / m^*$, and

$$C_d = L_0 e T / E_F. \quad (3)$$

The τ that appears here is the transport lifetime (though in the present sample it is unlikely that the transport and quantum lifetimes are significantly different since the electronic scattering is short range).

Zianni, Butcher, and Kearney⁵ rederive Eqs. (1) and (2) from Boltzmann's equation for the 2DEG. They also derive expressions for the phonon-drag contributions to \vec{S} , which we review here. Full details are given in the original paper.⁵ The predicted dependence of $S_{xx}^g(B)$ and $S_{yx}^g(B)$ on B is identical to that given above for the diffusive contributions to these elements of the thermopower tensor. Thus, we have

$$S_{xx}^g(B) = S_{xx}^g(0) + \Delta S_{xx}^g(B), \quad (4)$$

where

$$\Delta S_{xx}^g(B) = f_{xx} S_g^1 \frac{p\beta^2}{1+\beta^2}. \quad (5)$$

Here, S_g^1 is a function of T , which we discuss below. The Nernst-Ettingshausen coefficient is given by

$$S_{yx}^g(B) = -f_{yx} S_g^1 \frac{p\beta}{1+\beta^2}. \quad (6)$$

Zianni, Butcher, and Kearney⁵ find the theoretical value of both f_{xx} and f_{yx} to be 1. We will see from a comparison of these formulas with experimental data that indeed $f_{xx} = 1$ but $f_{yx} = 18.5$ for all T and B .

In the Appendix we show that

$$S_g^1 = [S_{xx}^g(0)]_{p=0} - [S_{xx}^g(0)]_{p=1}. \quad (7)$$

Consequently the programs used by Zianni, Butcher, and Kearney⁵ to evaluate $S_{xx}^g(0)$ can also be used to calculate S_g^1 . Then the total theoretical values of $S_{xx}(B)$ and $S_{yx}(B)$ are equal to the sums of the phonon-drag and electron-diffusion contributions.

IV. RESULTS AND DISCUSSION

A. Resistivity components

The field dependence of the resistivity at 4.2 K for another sample of the 2DEG from the same wafer has been given by Harris, Murray, and Foxon.⁶ Our measurements for the present sample are virtually identical. The resistivity is 1.30 k Ω at room temperature and changes by less than 0.2% down to about 80 K, below which it increases with decreasing T reaching about 1.43 k Ω by 4.2 K. This increase appears to be due to weak localization and this is also consistent with a decrease in ρ_{xx} with applied magnetic field, most of which occurs at $B < 1$ T. At 4.2 K, ρ_{xx} decreases to about 1.33 k Ω by 8 T and is still dropping slowly with increasing field.⁶ At 150 K, ρ_{xx} changes by less than 1% up to maximum field.

For a single band, $\rho_{yx} = -B/ne$. At 4.2 K the ratio B/ρ_{yx} is constant to within $\sim 0.3\%$ at magnetic fields up to 8 T and yields $n = 3.45 \times 10^{16} \text{ m}^{-2}$, with changes of no more than 2% on each cooldown. At 150 K, the magnitude of B/ρ_{yx} increases linearly with increasing B corresponding to a change in n from $(3.55-3.65) \times 10^{16} \text{ m}^{-2}$ as B is increased from near zero to 8 T. It is not clear why this happens. One possibility could be a small number of carriers thermally excited to the next subband, but the lack of any change in ρ_{xx} as a function of field or temperature appears to be inconsistent with this. Since we will be mainly interested in the mobility μ at higher fields, we will take $n = 3.6 \times 10^{16} \text{ m}^{-2}$ and $\rho = 1.30 \text{ k}\Omega$ to give $\mu = 0.13 \text{ m}^2/\text{V s}$.

B. Thermopower at zero magnetic field

Figure 1 shows the thermal conductivity λ measured when $B=0$. The phonon mean free path (mfp) l_p can be obtained by using the simple formula

$$\lambda = \frac{1}{3} C_v l_p v_s, \quad (8)$$

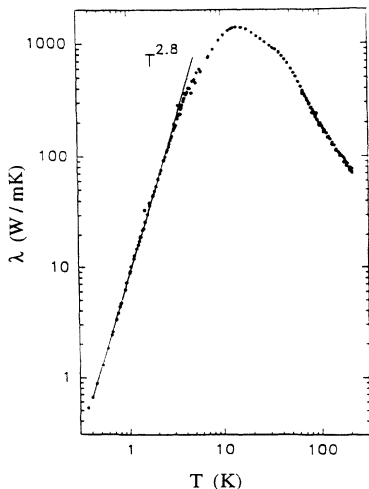


FIG. 1. The measured thermal conductivity λ of the substrate as a function of temperature T .

where v_s^{-3} is the average inverse cube speed of sound for the three acoustic modes.¹⁰ Using the values^{5,11} $v_T = 3040 \text{ m/sec}$ and $v_L = 5140 \text{ m/sec}$, for the acoustic transverse and longitudinal modes in GaAs, respectively, we estimate $v_s \approx 3368 \text{ m/sec}$. The phonon specific heat C_v in the Debye approximation for the three acoustic branches, is written in the form¹⁰

$$C_v = \frac{3}{2\pi^2} \left(\frac{k_B T}{\hbar v_s} \right)^3 k_B \int_0^{\theta_0/T} \frac{x^4 e^x}{(e^x - 1)^2} dx, \quad (9)$$

where $x = \hbar v_s Q / k_B T$ and Q is the magnitude of the phonon wave vector. The Debye temperature for GaAs in our calculations is $\theta_0 = 345 \text{ K}$.¹² The phonon mfp's calculated from the experimental data for λ are shown in Fig. 2 (open circles).

The thermopower measurements at zero magnetic field, $-S_{xx}(0)$, are shown in Fig. 3 (open circles) as a function of temperature. The straight line is the expected behavior of the diffusion component $S_{xx}^d(0)$, Eq. (2c), calculated in a way that will be described below; the data are seen to approach this line only at high temperatures. The peak in $-S_{xx}(0)$, with a maximum of about 330 $\mu\text{V/K}$ near 15 K, is caused by the phonon-drag component $-S_{xx}^g(0)$ and is very similar to, and has the same location as the peaks seen in three high-mobility samples² ($\mu \sim 19-62 \text{ m}^2/\text{V s}$). The peak magnitude in the high-mobility samples ranged from 400–1200 $\mu\text{V/K}$. These results should put to rest any suggestion that phonon drag is small for low-mobility samples.³

The increase of $-S_{xx}(0)$ at high temperatures is due to the linear dependence of the diffusion thermopower on T shown in Eqs. (2c) and (3). Information about both $S_{xx}^d(0)$ and $S_{xx}^g(0)$ may be derived by an appropriate analysis of this part of the plot of $S_{xx}(0)$ against T . We may write $-S_{xx}^d(0) = AT$, where A is a constant. Moreover, inspection of Eqs. (A1)–(A6) and (8) at high temperatures suggests that $-S_{xx}^g(0) = C\lambda$, where the temper-

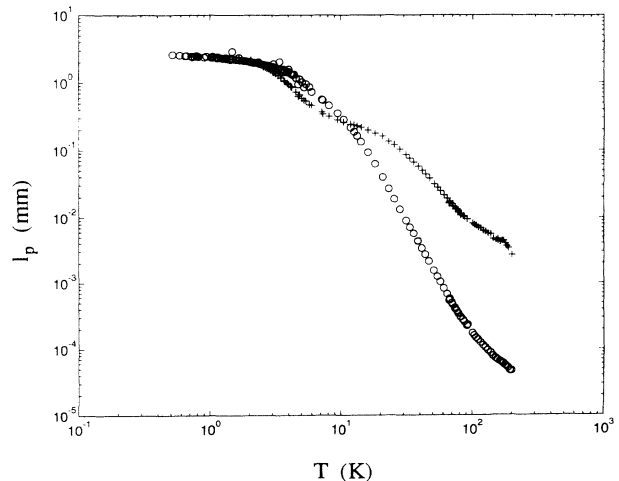


FIG. 2. The phonon mfp's calculated from λ (open circles) and from $S_{xx}(0)$ data (crosses) as described in the text.

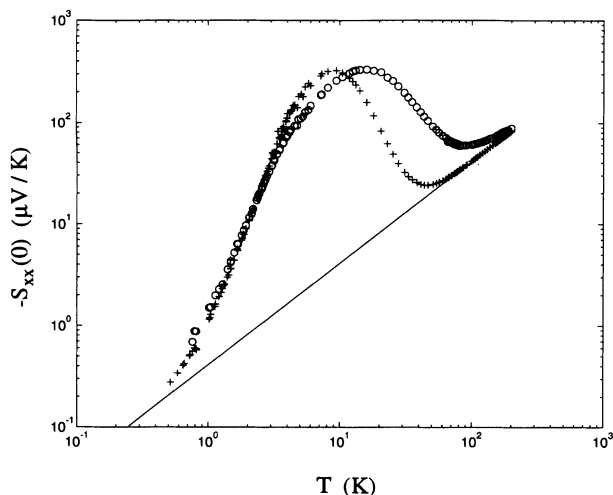


FIG. 3. The measured thermopower $-S_{xx}(0)$ as a function of temperature T (open circles) for the sample. The $S_{xx}(0)$ data were taken over a time period of about four months, but the individual data sets show no systematic variations from each other. In the same figure crosses show the theoretical values of $-S_{xx}(0)$ using the mfp's calculation from λ data as described in text. The straight line is the diffusion thermopower evaluated as explained in the text.

ature dependence of C can be neglected.¹³ Hence, $-S_{xx}(0) = AT + C\lambda$ and a plot of $-S_{xx}(0)/\lambda$ against T/λ should be a straight line with slope A and intercept C . We show such a plot in Fig. 4 for $T > 65$ K. Our expectations are confirmed and we find that $A = 0.41 \mu\text{V}/\text{K}^2$ with an error of $\pm 1\%$ (this uncertainty does not include that due to the thermometer spacing of about 5%). The straight line in Fig. 3 is a plot of $S_{xx}^d(0) = -0.41T \mu\text{V}/\text{K}$. In Fig. 3 we also show the theoretical estimates of $-S_{xx}(0)$ (crosses) as the sum of the diffusive contribution AT and the drag contribution. The drag part is calculated using the average phonon mfp derived from the thermal-conductivity data and standard GaAs parameters where required.⁵ We see from Fig. 3 that it rapidly approaches zero above 70 K.

At this point we should note that the value for the acoustic-phonon deformation potential E_1 for GaAs is

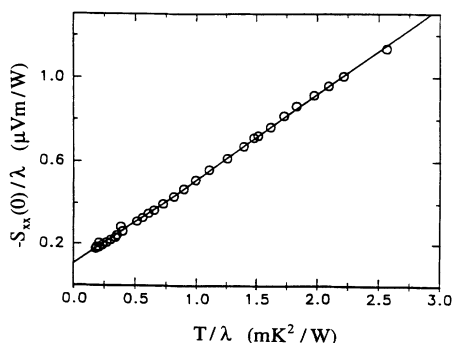


FIG. 4. The empirical ratio $S_{xx}(0)/\lambda$ as a function of T/λ over the temperature range 66–200 K.

uncertain. In the literature the values for E_1 range from 7 to 16 eV. However, in our case the best fitting of $S_{xx}(0)$ to experiment occurs for Lyo's¹¹ suggested value $E_1 = 9.3$ eV. Moreover, GaAs is piezoelectric and E_1^{eff} in Eq. (A6) includes the effect of the piezoelectric coupling with the piezoelectric coefficient $h_{14} = 1.2 \times 10^9 \text{ V m}^{-1}$. Details are given in Ref. 5. We see from Fig. 3 that, in general, the theory⁵ predicts reasonably well the behavior of $S_{xx}(0)$ as a function of temperature. At lower temperatures ($T < 10$ K), the theoretical values of the total thermopower are in good agreement with the corresponding experimental ones. The agreement is extremely good for $T < 3.5$ K. This is a good indication that in this temperature regime the boundary scattering assumption works very well. However, above 20 K the predicted thermopower becomes up to an order of magnitude smaller than the data. The reason is that different average mfp's are involved in λ and $S_{xx}^g(0)$.¹⁴ More specifically, for $T > 20$ K the phonons that contribute to λ seem to be characterized by up to an order of magnitude smaller mfp's than the phonons that contribute to $S_{xx}^g(0)$.

Our other main concern here is the behavior of the magnetothermopower $\Delta S_{xx}(B)$ and the Nernst-Ettingshausen coefficient $S_{yx}(B)$. To avoid introducing errors via the phonon mfp's into the theoretical formulas for these quantities, we determine the phonon mfp's from the $S_{xx}(0)$ data (subtracting the diffusive part first) using Eqs. (A1) and (A3). Then the agreement of the calculated values of $S_{xx}(0)$ with the data is automatic. The phonon mfp's calculated from the phonon-drag contribution, $S_{xx}^g(0)$, are shown in Fig. 2 (crosses). The difference from the corresponding phonon mfp's estimated from λ data (open circles in the same figure) is obvious.

Finally, and perhaps most importantly, given $A = 0.41 \mu\text{V}/\text{K}^2$ with an error of $\pm 1\%$, it is possible to calculate the parameter p in Eq. (2) for the diffusive thermopower. Taking the effective mass¹⁵ $m^* = 0.07m_e \pm 5\%$ (it is not clear how large the nonparabolic band effects are for such a high-density sample) and the electron density $n = 3.6 \times 10^{16} \text{ m}^{-2}$ with an error of $\pm 3\%$, we obtain $L_0 e / E_F = 0.198 \mu\text{V}/\text{K}^2$ with an error of $\pm 6\%$ so that, from Eqs. (2c) and (3) we have $p = 1.07 \pm 15\%$. In this large uncertainty for p are included the thermometer-spacing error as well as that in m^* and n . Excluding all these extra errors and keeping only the statistical uncertainty in A ($\pm 1\%$), p is found to be uncertain to about $\pm 2\%$. There is no published theory that gives this quantity for the present sample. The closest value is that of Karavolas and Butcher,¹⁶ which is about 1.0 for the case of background (i.e., short range) impurities in a GaAs/Ga_{1-x}Al_xAs quantum well when $n \sim 1 \times 10^{16} \text{ m}^{-2}$.

C. Results in a magnetic field

Measurements on S_{yx} and S_{xx} were made as a function of magnetic field over the whole temperature range 1–200 K. Further data on $S_{yx}(B)$ were obtained at many more temperatures from averages at a fixed field of ± 7.3 T. These latter are shown in Fig. 5 (open circles) and the

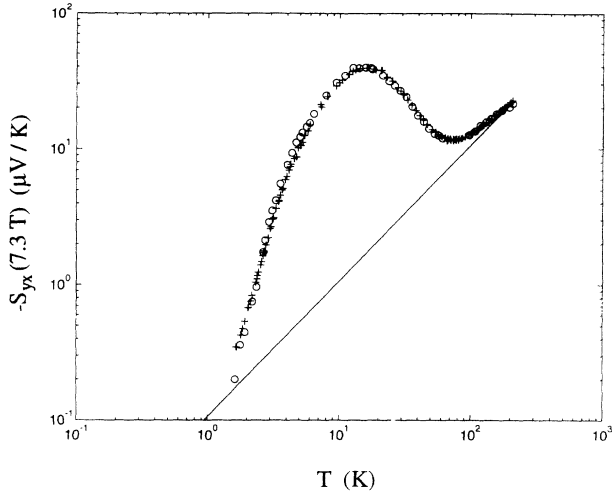


FIG. 5. The variation of $-S_{yx}(B)$ at a fixed field of 7.3 T as a function of temperature T (open circles); the data are suitable averages of $\pm B$ results. The straight line is the diffusion contribution calculated for $p=1.07$. The crosses denote the calculated values of $-S_{yx}(B)$ using the parameters $p=1.07$, $\mu=0.13$ $\text{m}^2/\text{V s}$, and $f_{yx}=18.5$.

general behavior is seen to be similar to that for $S_{xx}(0)$ shown in Fig. 3. At lower temperatures the two figures superimpose reasonably closely except for a scaling factor. This shows that $S_{yx}(B)$ is dominated by phonon drag up to ~ 50 K. These results provide an unambiguous demonstration of the presence of phonon drag in this coefficient, though high-field data in the quantum Hall and fractional quantum Hall regime have pointed in the same direction (e.g., Refs. 1 and 17).

The straight line in Fig. 5 is the diffusion contribution to the Nernst-Ettingshausen coefficient [Eq. (2d)] at $B=7.3$ T calculated for $\mu=0.13$ $\text{m}^2/\text{V s}$ and taking $p=1.07$ as previously estimated from $S_{xx}(0)$ and λ data. It approaches the data points at the highest temperatures considered. This behavior is consistent with the dominance of $S_{yx}(B)$ by electron diffusion at these temperatures and confirms that $p=1.07$ in $S_{yx}^d(B)$ as well as in $S_{xx}^d(0)$.

To determine f_{yx} in Eq. (6) we adjust it to secure agreement between the theoretical and experimental values of $S_{yx}(B)$ at $B=7.3$ T for all T . With $f_{yx}=18.5$, $p=1.07$, $\mu=0.13$ $\text{m}^2/\text{V s}$, and S_g^1 calculated from Eq. (7) using the same GaAs parameters as those for the calculation of $S_{xx}^g(0)$, the theoretical results are shown as crosses in Fig. 5. We see that the agreement between theory and experiment is extremely good.

Some of the field sweeps for $-S_{yx}(B)$ at various temperatures are shown in Fig. 6 (these are averages from $\pm B$ sweeps). The data are linear in B at low fields and tend to approach maxima at the highest fields, in qualitative agreement with the B dependencies of $-S_{yx}^d(B)$ and $-S_{yx}^g(B)$ in Eqs. (2d) and (6), respectively. The curves drawn in Fig. 6 are calculated from the above equations with $f_{yx}=18.5$ and S_g^1 calculated in the same manner as before. We adjust p and μ at each temperature to get the

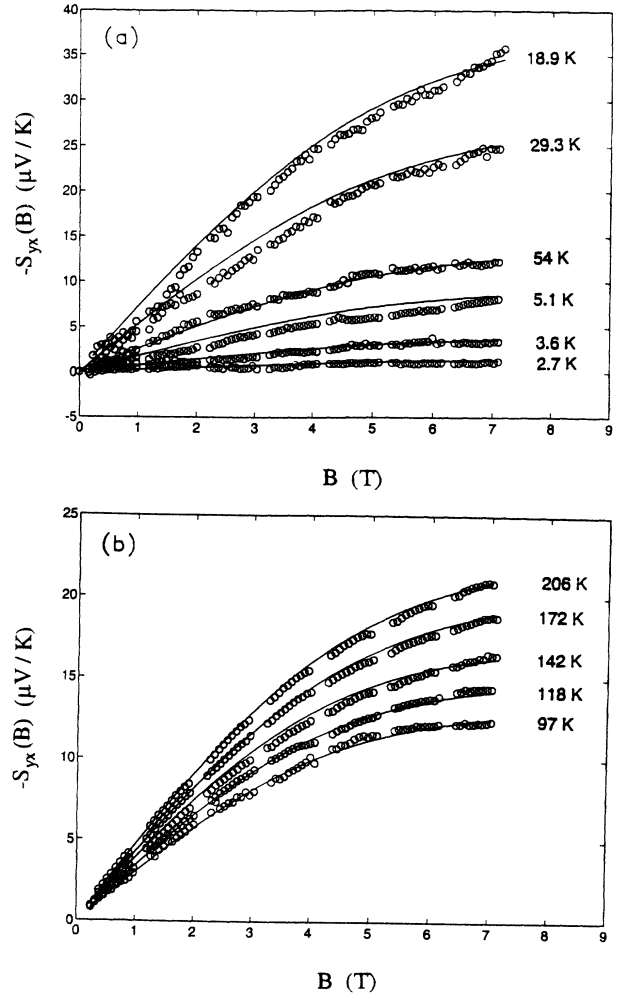


FIG. 6. The variation of $S_{yx}(B)$ with field B at various temperatures; the data are suitable averages of $\pm B$ results. The curves are fitted as described in the text. For clarity, the data have been separated into two groups. (a) Low temperatures where phonon drag is dominant (except for the plot at 54 K, where diffusion and phonon drag are similar). (b) High temperatures where diffusion is dominant. The values of p and μ , used at any temperature, are given in the text. The overall mean values of these two quantities of the $S_{yx}(B)$ fit for all the temperatures, are $p=1.02\pm 0.02$ and $\mu=0.107\pm 0.003$ $\text{m}^2/\text{V s}$.

best fit. For the lower-temperature regime [Fig. 6(a)], as T changes from 2.7 to 18.9 K, the appropriate values for p are 0.91, 0.91, 0.91, 1.03, 1.07, and 1.07, respectively. The corresponding μ value is 0.10 $\text{m}^2/\text{V s}$ for all the temperatures. In the same manner, for higher temperatures [Fig. 6(b)], as the temperature rises the chosen values for p are 1.07 for all the temperatures apart from $T=206$ K, for which $p=1.03$. The corresponding values for the mobility are 0.12, 0.12, 0.12, 0.11, and 0.11 $\text{m}^2/\text{V s}$. Since we assume that there is no dependence of p and μ on temperature or field we estimate the overall mean value of these two quantities, from the above $-S_{yx}(B)$ fit, to be $p=1.02\pm 0.02$ and $\mu=0.107\pm 0.003$ $\text{m}^2/\text{V s}$. This value of p is in very good agreement with that p obtained from the $-S_{xx}(0)$ fit for high temperatures, which is

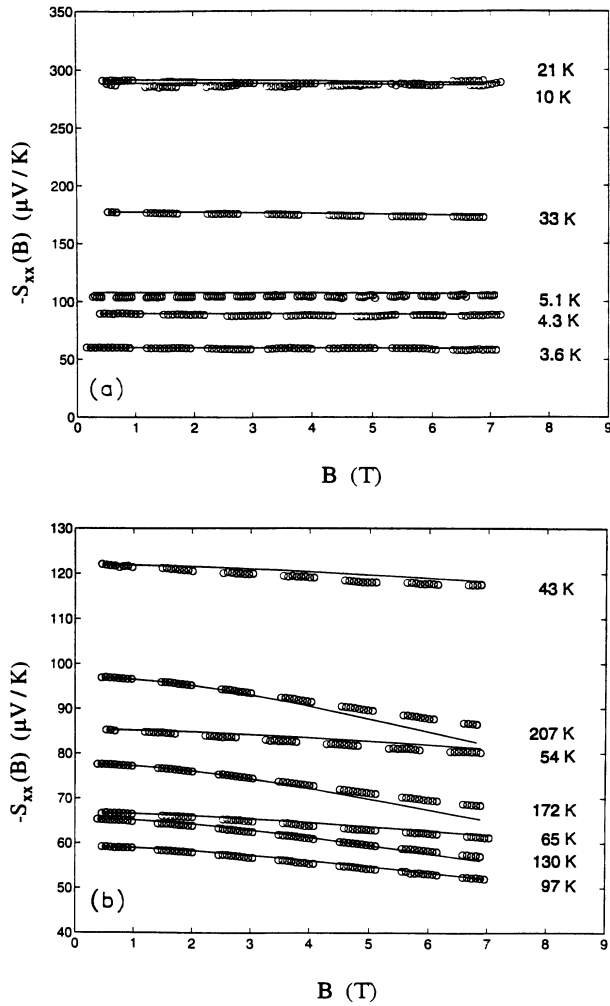


FIG. 7. The variation of the thermopower $-S_{xx}(B)$ as a function of magnetic field B at various temperatures. (a) Data at low temperatures where phonon drag dominates. (b) Data at higher temperatures, where diffusion effects are significant and cause a decrease in $-S_{xx}(B)$ with B . All the solid curves are calculated for $f_{xx} = 1$, $p = 1.02$, and $\mu = 0.107 \text{ m}^2/\text{V s}$.

$1.07 \pm 2\%$. The calculated mobility is also in fair agreement with the measured value: $\mu = 0.13 \text{ m}^2/\text{V s}$.

Finally, we turn our attention to $S_{xx}(B)$ in Fig. 7. The open circles show the experimental data and the curves are calculated from Eqs. (2a), (2b), (4), and (5), with $f_{xx} = 1$. S_g^1 is calculated in the same manner as before and p and μ are the mean values calculated above. For low temperatures, $\Delta S_{xx}(B)$ is negligible in comparison with $S_{xx}(0)$ and so good agreement is ensured [Fig. 7(a)]. For the high-temperature curves, shown in Fig. 7(b), we again obtain very good agreement between theory and experiment (the maximum difference which is observed is $\sim 4.5\%$ for $T = 172$ and 207 K), which provides another test of the theory.

V. CONCLUSIONS

The experimental results that we have presented on the thermoelectric behavior of a very-low-mobility 2DEG

show relatively simple behavior. The zero-field drag thermopower $-S_{xx}^g(0)$ quite closely resembles the experimental thermal conductivity λ , given in Fig. 1, for $T > 65 \text{ K}$. Nevertheless, there is a significant difference between the average phonon mean paths derived from λ and $S_{xx}^g(0)$. The next step in understanding both λ and $S_{xx}^g(0)$ and their relationship is to develop the microscopic theory further so as to introduce realistic dependencies of the mfp on the phonon wave vector. In this paper we have avoided the problem by calculating the average mfp from $S_{xx}^g(0)$ and concentrating most of our attention on the magnetothermopower $\Delta S_{xx}(B)$ and the Nernst-Ettingshausen coefficient $S_{yx}(B)$. The theory of these quantities developed recently by Zianni, Butcher, and Kearney⁵ yields dependencies on $\beta = \mu B$ for the phonon-drag contributions to $\Delta S_{xx}(B)$ and $S_{yx}(B)$, which are the same as those found in the standard theory of the diffusive contributions. Moreover, the theoretical behavior of $S_{xx}(B)$ is in reasonable agreement with the observed behavior when $T \leq 200 \text{ K}$ and $B \leq 8 \text{ T}$. Where the theory is seriously at fault is in the determination of $S_{yx}(B)$. It gives $S_{yx}(B) = \Delta S_{xx}(B) / \mu B$. This relation is well known for the diffusion contributions to these quantities. Zianni, Butcher, and Kearney⁵ find the same relation between the phonon-drag contributions and, therefore, between the total $S_{yx}(B)$ and $\Delta S_{xx}(B)$. The experimental data, however, are consistent with $S_{yx}^g(B) = 18.5 \Delta S_{xx}^g(B) / \mu B$. The origin of the constant factor of 18.5 in this relationship is not known. It is much more likely to be due to an oversimplification of the theoretical model than to some undetected experimental error. This factor apart, the theory is in good agreement with the experimental data for the wide ranges of B and T investigated.

ACKNOWLEDGMENTS

This work was supported by a grant from the Natural Sciences and Engineering Research Council of Canada and the Science and Engineering Research Council of the U.K.

APPENDIX: THE RELATIONSHIP BETWEEN $S_{xx}^g(0)$ AND S_g^1

Zianni, Butcher, and Kearney⁵ give the following formulas for $S_{xx}^g(0)$ and S_g^1 :

$$S_{xx}^g(0) = -\frac{2\tau}{\sigma_0} I_0 \quad (\text{A1})$$

and

$$S_g^1 = \frac{2\tau}{\sigma_0} I_1, \quad (\text{A2})$$

where σ_0 and τ are the zero-field conductivity and the relaxation time at the Fermi level. In these equations

$$I_0 = \int \int dq dq_z C_g q^2 F(\mathbf{Q}) \lambda^0(\mathbf{Q}) J(\mathbf{Q}) \quad (\text{A3})$$

and

$$I_1 = \int \int dq dq_z C_g q^2 F(\mathbf{Q}) \lambda^1(\mathbf{Q}) J(\mathbf{Q}), \quad (\text{A4})$$

where

$$\lambda_0 = 1 + p\lambda^1(\mathbf{Q}) \quad (\text{A5})$$

and

$$C_g = \frac{el_p(2m^*)^{1/2}(E_1^{\text{eff}})^2}{32\pi^3\hbar k_B T^2 \rho} \quad (\text{A6})$$

In these equations m^* is the electron effective mass, ρ is the density of the material, and l_p is the phonon mfp's. Moreover, as we mentioned in the text, since GaAs is piezoelectric, the term $(E_1^{\text{eff}})^2$ denotes the sum of the

acoustic deformation-potential contribution, E_1^2 , and the piezoelectric contribution to the total electron-phonon interaction. The analytical expression for the piezoelectric interaction for LA and TA modes and full notational details are given in the original paper.⁵

We see by inspection that I_1 is obtained from I_0 by replacing λ_0 by

$$\lambda_1 = (\lambda_0 - 1)/p \quad (\text{A7})$$

Hence it follows from Eqs. (A1) and (A2) that

$$S_g^1 = [S_{xx}^g(0)]_{p=0} - [S_{xx}^g(0)]_{p=1} \quad (\text{A8})$$

- ¹B. L. Gallagher and P. N. Butcher, in *Handbook on Semiconductors*, edited by P. T. Landsberg (Elsevier, Amsterdam, 1992), Vol. 1, p. 817.
- ²B. R. Cyca, R. Fletcher, and M. D'Iorio, *J. Phys. Condens. Matter* **4**, 4491 (1992).
- ³C. Ruf, H. Obloh, B. Junge, E. Gmelin, K. Ploog, and G. Weimann, *Phys. Rev. B* **37**, 6377 (1988).
- ⁴V. I. Fal'ko and S. V. Iordanskii, *J. Phys. Condens. Matter* **4**, 9201 (1992).
- ⁵X. Zianni, P. N. Butcher, and M. J. Kearney, *Phys. Rev. B* **49**, 7520 (1994).
- ⁶J. J. Harris, R. Murray, and C. T. Foxon, *Semicond. Sci. Technol.* **8**, 31 (1993).
- ⁷M. G. Holland, *Phys. Rev.* **134**, A471 (1964).
- ⁸S. A. Aliev and S. S. Shalyt, *Fiz. Tverd. Tela* **7**, 3690 (1965)

[*Sov. Phys. Solid State* **7**, 2986 (1966)].

- ⁹R. S. Averback and D. K. Wagner, *Solid State Commun.* **11**, 1109 (1972).
- ¹⁰N. W. Ashcroft and N. D. Mermin, *Solid State Physics* (SCP, New York, 1976).
- ¹¹S. K. Lyo, *Phys. Rev. B* **38**, 6345 (1988).
- ¹²C. W. Garland and K. C. Park, *J. Appl. Phys.* **33**, 759 (1962).
- ¹³M. J. Smith and P. N. Butcher, *J. Phys. Condens. Matter* **2**, 2375 (1990).
- ¹⁴E. Behnen, *J. Appl. Phys.* **67**, 287 (1990).
- ¹⁵M. A. Hopkins, R. J. Nicholas, M. A. Brummel, J. J. Harris, and C. T. Foxon, *Phys. Rev. B* **36**, 4789 (1987).
- ¹⁶V. C. Karavolas and P. N. Butcher, *J. Phys. C* **3**, 2597 (1991).
- ¹⁷U. Zeitler, J. C. Maan, P. Wyder, R. Fletcher, C. T. Foxon, and J. J. Harris, *Phys. Rev. B* **47**, 16008 (1993).